

Case Report

F-18 FDG hypermetabolism in mass-forming focal pancreatitis and old hepatic schistosomiasis with granulomatous inflammation misdiagnosed by PET/CT imaging

Song Ye¹, Wei-Lin Wang¹, Kui Zhao²

Departments of ¹Hepatobiliary and Pancreatic Surgery, ²PET/CT Center, The First Affiliated Hospital, College of Medicine, Zhejiang University, Zhejiang 310003, China

Received July 26, 2014; Accepted August 23, 2014; Epub August 15, 2014; Published September 1, 2014

Abstract: Purpose: We report the case of a 59-year-old male patient who presented with space-occupying lesions in the pancreas and liver suggestive of metastatic pancreatic cancer. Materials and methods: Whole-body F-18 fluorodeoxyglucose (FDG) PET/CT imaging and enhanced CT imaging of the lesions were performed in addition to abdominal ultrasound, ERCP, and MRCP. Tumor markers, including CA199 and AFP, were also evaluated. Results: PET/CT imaging showed a soft tissue mass with indistinct boundaries in the head of the pancreas with a maximum SUV of 4.39. A less dense shadow was also found in the left lobe of the liver with an indistinct boundary and a maximum SUV of 4.13. Enhanced CT revealed an enhancing mass in the head of the pancreas on arterial phase imaging as well as a mildly enhancing focus in the left lobe of the liver. The patient was diagnosed with a space-occupying lesion of the uncinate process of the pancreas suggestive of pancreatic cancer with metastasis to the liver. However, serum tumor markers were normal. Postoperative pathology was consistent with chronic pancreatitis and old hepatic schistosomiasis associated with granulomatous inflammation of the liver. Conclusion: This case of mass-forming pancreatitis and granulomatous inflammation in old hepatic schistosomiasis mimicked metastatic pancreatic cancer on PET/CT. Such false positive lesions have not been reported before, and further exploration and investigation are needed.

Keywords: Pancreatic carcinoma, mass-forming pancreatitis, PET/CT, granulomatous, liver metastasis, schistosome

Introduction

Whole-body F-18 fluorodeoxyglucose (FDG) PET/CT imaging not only makes early detection of primary tumors possible but also allows the extent of disease throughout the body to be evaluated [1-3]. There have been numerous studies on the application of F-18 FDG PET to the diagnosis of pancreatic lesions [4, 5]. Unfortunately it is not tumor specific. Herein, we present a case of mass-forming pancreatitis with false positive findings on CT, MRI, ERCP, US, and PET/CT suggestive of pancreatic cancer.

Case report

A 59-year-old male patient was admitted to our hospital because of dark urine for more than

10 days and was found to have space-occupying lesions in the pancreas and liver. His medical/surgical history showed a bout of hepatic schistosomiasis 30 years previously and prostate surgery in September 2009. On physical examination, mild jaundice of the sclera, but no significant jaundice of the skin, was noted. The abdomen was soft, and a surgical scar, approximately 15 cm in length, was seen in the lower abdomen, but there was no rebound tenderness. No obvious mass was palpitated, the liver and spleen were not palpitated under the costal arch, and Murphy's sign was negative.

Laboratory tests included the following: total bile acids 1168.6 $\mu\text{mol/l}$, total bilirubin 71.3 $\mu\text{mol/l}$, direct bilirubin 25.7 $\mu\text{mol/l}$, indirect bilirubin 45.67 $\mu\text{mol/l}$, total protein 84.5 g/l, albumin 41.7 g/l, glutamic-pyruvic transaminase

PET/CT imaging of pancreatitis and old hepatic schistosomiasis

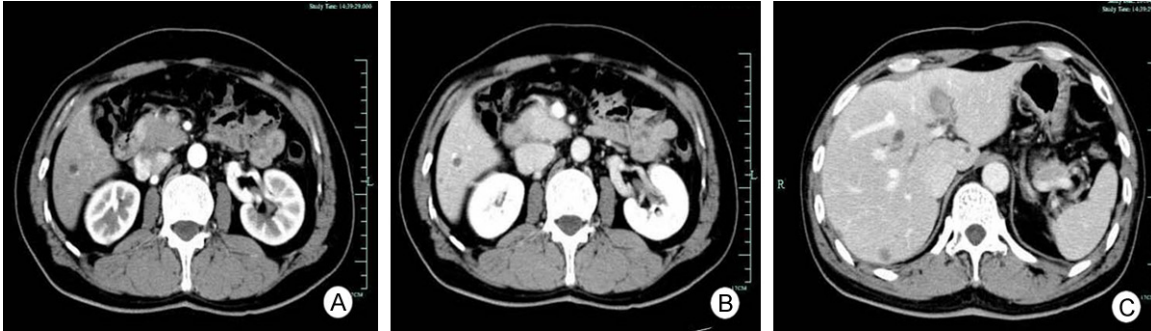


Figure 1. Cross-sectional enhanced CT images. A, B. An enhancing mass in the head of the pancreas on arterial-phase imaging. C. A small mildly enhancing low-density focus in the left lobe of the liver.

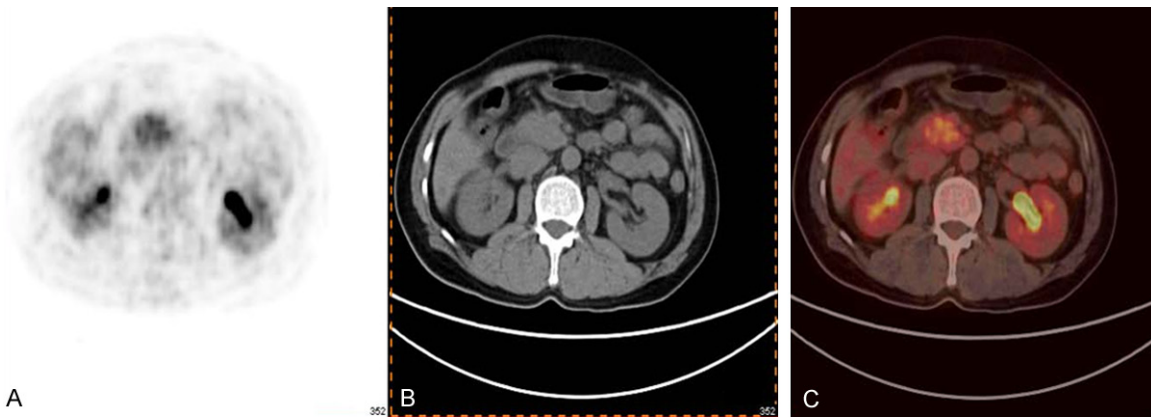


Figure 2. Cross-sectional PET/CT imaging. A. PET scan image. B. Plain CT image. C. Merged PET/CT image. These images show a 4.20 × 2.81-cm soft tissue mass with unclear boundaries in the head of the pancreas. It measured 42 HU on CT, with a maximum SUV of 4.39 on PET.

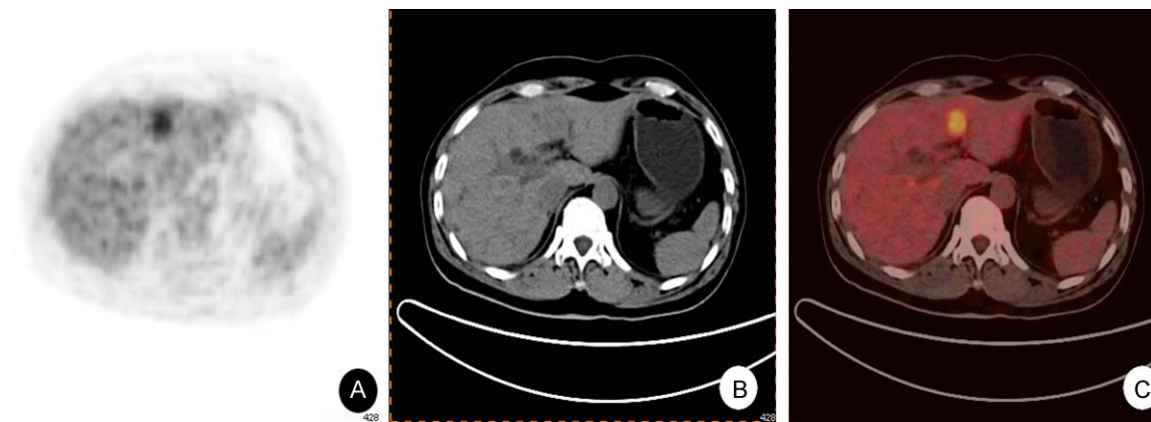


Figure 3. Cross-sectional PET/CT imaging. A. PET scan image. B. Plain CT image. C. Merged PET/CT image. These images show a 1.54 × 2.42-cm low-density mass with unclear boundaries in the left lobe of the liver, with a maximum SUV of 4.13 on PET.

277 IU/L, glutamic-oxalacetic transaminase 140 IU/L, and γ -glutamyl transpeptidase 654 IU/L. Tumor markers, including CA199 (3.1 U/l) and AFP (4.1 ng/ml), were normal.

Abdominal ultrasound showed diffuse liver disease with many hypoechoic lesions throughout the liver, and a space-occupying lesion in the left lobe of the liver suggestive of metastasis. A

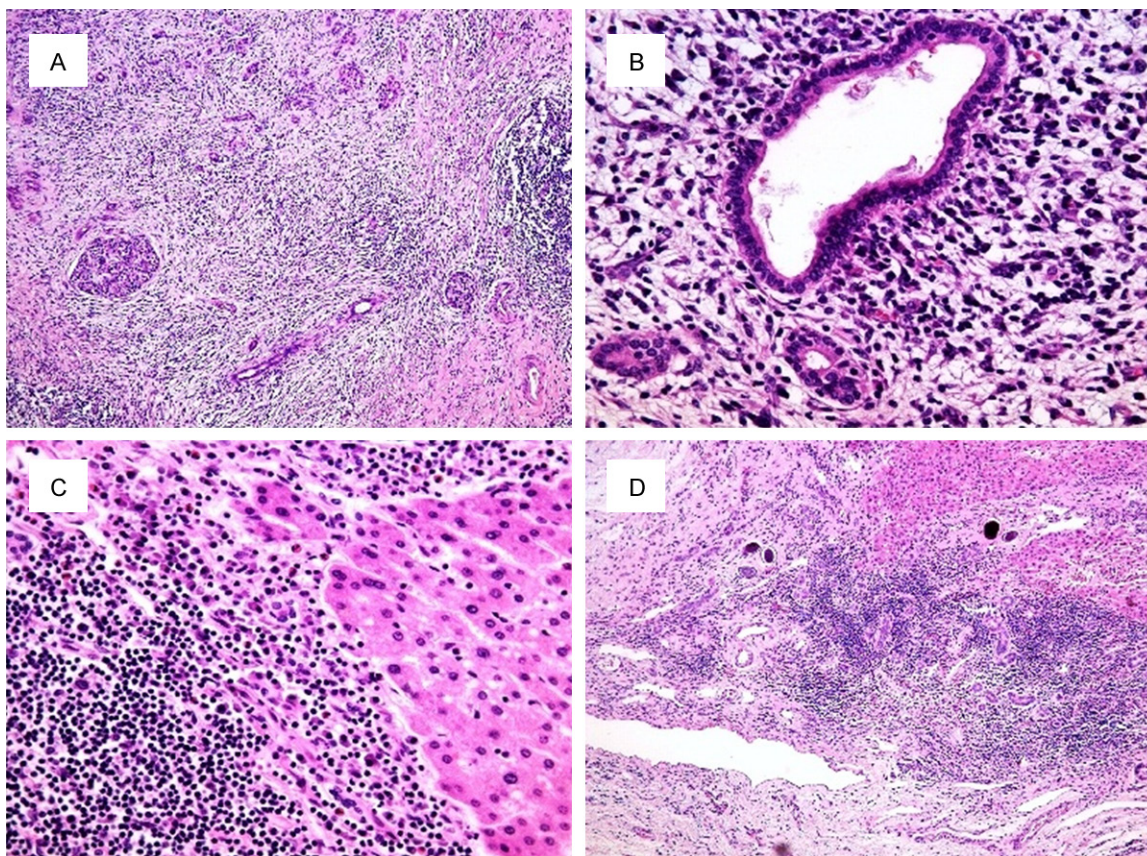


Figure 4. A. Atrophy of pancreatic acinar cells, proliferation of interstitial fibrous tissue, inflammatory cell infiltration, and the presence of remnant islets (HE, 100 ×). B. Significant infiltration of numerous inflammatory cells around the pancreatic duct. C. Significant infiltration of inflammatory cells and fibrous tissue proliferation in the liver (HE, 400 ×). D. Deposition of schistosome eggs in the liver and infiltration of a large number of inflammatory cells.

space-occupying lesion was also noted in the head of the pancreas and the common bile duct was slightly dilated, suggesting pancreatic cancer.

A preoperative CT scan showed a mass in the uncinate process of the pancreas which enhanced on arterial phase imaging, as well as an additional mildly enhancing low-density focus (**Figure 1**) in the left medial segment of the liver and right hepatic cysts.

MRCP showed that the structure of the biliary tree was normal with no dilation or stenosis of the intrahepatic bile duct, the common hepatic duct, or the middle or upper segments of the common bile duct. In the left liver, another branch of the bile duct was found to enter the common hepatic duct at a low position, and the inferior segment of the common bile duct was thinned and beak-like upon entering the duodenum. The pancreatic duct appeared partially

thinned in the region of the head of the pancreas.

Whole-body FDG PET/CT imaging showed a soft tissue mass measuring 4.20 × 2.81 cm with unclear boundaries in the head of the pancreas. The mass measured 42 HU on CT, with a maximum SUV of 4.39 (**Figure 2**) on PET. No abnormality was observed in the pancreatic body or tail, and no significant dilation was found in the pancreatic duct. There was a 1.54 × 2.42-cm low-density lesion with unclear boundaries in the left lobe of the liver with a maximum SUV of 4.13 (**Figure 3**) on PET. There were multiple low-density cystic lesions within the liver, the largest measuring 1.25 cm. No adenopathy was seen in the retroperitoneum.

Our initial diagnosis was probable pancreatic cancer in the uncinate process of the pancreas with metastasis to the left lobe of the liver. After discussion, we decided to carry out a

biopsy to obtain a more accurate diagnosis before deciding on a treatment strategy. However, the patient refused biopsy and requested immediate surgical treatment. Therefore, we carried out pancreatoduodenectomy together with child's reconstruction and left hepatectomy in August 2010 under general anesthesia. Intraoperative sonography further suggested a malignant tumor in the head of the pancreas with metastasis to the left lobe of the liver. During surgery, a hard mass measuring approximately 3 cm was excised from segment IVb of the left liver. A 3 × 4-cm hard mass was also removed from the uncinata process of the pancreas. Several enlarged lymph nodes were removed from the retroperitoneum. No significant space-occupying lesion was found in any other organ in the abdominal or pelvic cavity, and there was no ascites.

Pathological examination of the gallbladder, which was excised during the Whipple procedure, showed chronic inflammatory changes. No metastatic change was found in the one lymph node harvested from the gallbladder neck or in the four lymph nodes harvested from the hepatic portal region. The final pathology report was compatible with chronic cholecystitis without metastatic changes in the lymph nodes of the hepatic portal region.

Pathological examination of the 3 × 4-cm mass harvested from the pancreas during the Whipple procedure was consistent with chronic pancreatitis associated with significant proliferation of fibrous tissue. Microscopically, atrophy of pancreatic acinar cells, proliferation of interstitial fibrous tissue, and infiltration of inflammatory cells were found in the pancreatic mass (**Figure 4**).

On microscopy, the 3.5 × 2.5 × 1.5-cm liver mass showed nodular proliferation of fibrous tissue, infiltration of lymphocytes and plasma cells, and old deposition of schistosome eggs. These findings were compatible with old hepatic schistosomiasis associated with granulomatous inflammation (**Figure 4**).

Discussion

Pancreatic cancer grows relatively rapidly, with frequent early metastasis. Most patients are in the late stage of the disease when diagnosed [6, 7]. The diverse clinical manifestations of

pancreatic cancer are related to tumor location, disease stage, the relationship with peripheral tissues, and the presence or absence of metastasis. The key to improving therapeutic outcomes is early diagnosis. However, there are no typical symptoms at early stages, which render diagnosis difficult. Although tumor markers such as CA199 and CEA can guide therapy, they lack specificity. Imaging techniques including CT, MRI, endoscopic ultrasound, ERCP, MRCP, and fine-needle aspiration biopsy (FNAB) are essential to accurate diagnosis and therapy. Among them, CT is the most commonly used technique for diagnosing pancreatic cancer and for preoperative evaluation [8, 9].

Whole-body FDG PET/CT imaging not only makes early detection of primary tumors possible but also allows the extent of disease throughout the body to be evaluated [1-3]. It is relatively accurate in N and M staging of pancreatic cancer, and often uncovers more metastases compared to other imaging modalities, providing an objective basis for accurate staging and selection of treatment methods [10, 11].

There have been numerous studies on the application of F-18 FDG PET to the diagnosis of pancreatic lesions [4, 5]. Most reported that FDG PET was more accurate than CT. The sensitivity of CT in the diagnosis of pancreatic cancer increases with increased lesion volume, while the sensitivity of FDG PET is not related to lesion size [4, 11]. PET/CT also integrates anatomical imaging and functional imaging. It not only effectively evaluates the metabolism, proliferation, hypoxia, and tissue apoptosis of the tumor but also accurately shows the anatomical structure between the tumor and adjacent organs. Therefore, it has significant prognostic value in the diagnosis and staging of pancreatic cancer [12].

In the present study, preoperative PET/CT showed a 4.20 × 2.81-cm soft tissue mass with unclear boundaries in the head of the pancreas that was hypermetabolic on PET, with a maximum SUV of 4.39. This presentation is similar to the FDG metabolic profile of pancreatic cancer. Moreover, enhanced CT showed a mass in the head of the pancreas on arterial phase imaging and a mildly enhancing low-density focus in the left liver. Because the liver is the

most common location of systemic metastasis from pancreatic cancer [10], liver metastasis from pancreatic cancer was our first consideration. However, the pancreatic mass was misdiagnosed as pancreatic cancer since the pathology was consistent with mass-forming pancreatitis. Differential diagnosis between pancreatic cancer and mass-forming pancreatitis has always been difficult, with a certain percentage of false positive results.

Additionally, we found a 1.54 × 2.42-cm low-density lesion with unclear boundaries in the left lobe of the liver. It was hypermetabolic on PET, with a maximum SUV of 4.13, and we considered it to be a liver metastasis. Pathological examination showed nodular proliferation of fibrous tissue, infiltration of lymphocytes and plasma cells, and old deposition of schistosome eggs. These changes were consistent with a granulomatous lesion misdiagnosed as liver metastasis. Though there have been reports about intestinal schistosomiasis granulomas, there has been no report of deposition of schistosome eggs associated with proliferation of inflammatory granulomatous tissue and PET/CT FDG hypermetabolism. Although the patient had suffered from schistosomiasis 30 years previously, there was no recent history of infection. Therefore, the reason for granulomatous inflammation at the site of schistosome egg deposition in the liver is not yet clear, and further studies are needed. The liver mass was a false positive lesion that mimicked the FDG hypermetabolism seen in liver metastases. The hypermetabolism might be related to proliferation of the granuloma.

In summary, we have presented a case of mass-forming pancreatitis with false-positive findings on CT, MRI, ERCP, US, and PET/CT suggestive of pancreatic cancer. Since the results of these auxiliary examinations could not be ignored, minimally invasive biopsy was the safest choice in this case, since no other method, including tumor marker assessment, could provide a clear diagnosis. When the tumor marker CA199 is not elevated in cases involving a pancreatic mass, pancreatic cancer should be differentiated from mass-forming pancreatitis. There has been no similar report on PET FDG hypermetabolism in hepatic granulomatous lesions from old schistosomiasis, which therefore requires further study.

Disclosure of conflict of interest

None.

Address correspondence to: Dr. Kui Zhao, Department of PET/CT Center, The First Affiliated Hospital, College of Medicine, Zhejiang University, 310003, China. Tel: 86-57187236428; Fax: 86-571-87236228; E-mail: zhaokuizh@163.com

References

- [1] Izuishi K, Yamamoto Y, Sano T, Takebayashi R, Nishiyama Y, Mori H, Masaki T, Morishita A and Suzuki Y. Molecular mechanism underlying the detection of colorectal cancer by 18F-2-fluoro-2-deoxy-D-glucose positron emission tomography. *J Gastrointest Surg* 2012; 16: 394-400.
- [2] Zhao K, Luo XM, Zhou SH, Liu JH, Yan SX, Lu ZJ, Yang SY, Lin LL and Dong MJ. ¹⁸F-fluorodeoxyglucose positron emission tomography/computed tomography as an effective diagnostic workup in cervical metastasis of carcinoma from an unknown primary tumor. *Cancer Biother Radiopharm* 2012; 27: 685-693.
- [3] Zhao K, Yang SY, Zhou SH, Dong MJ, Bao YY and Yao HT. Fluorodeoxyglucose uptake in laryngeal carcinoma is associated with the expression of glucose transporter-1 and hypoxia-inducible-factor-1 α and the phosphoinositide 3-kinase/protein kinase B pathway. *Oncol Lett* 2014; 7: 984-990.
- [4] Otomi Y, Otsuka H, Terazawa K, Nose H, Kubo M, Matsuzaki K, Ikushima H, Bando Y and Harada M. Comparing the performance of visual estimation and standard uptake value of F-18 fluorodeoxyglucose positron emission tomography/computed tomography for detecting malignancy in pancreatic tumors other than invasive ductal carcinoma. *J Med Invest* 2014; 61: 171-179.
- [5] Imperiale A, Rust E, Gabriel S, Detour J, Goichot B, Duclos B, Kurtz JE, Bachellier P, Namer IJ and Taïeb D. 18F-fluorodihydroxyphenylalanine PET/CT in patients with neuroendocrine tumors of unknown origin: relation to tumor origin and differentiation. *J Nucl Med* 2014; 55: 367-372.
- [6] Siegel R, Ma J, Zou Z and Jemal A. Cancer statistics, 2014. *CA Cancer J Clin* 2014; 64: 9-29.
- [7] Baiocchi GL, Portolani N, Grazioli L, Mazza G, Gheza F, Bartoli M, Vanzetti E and Giulini SM. Management of pancreatic intraductal papillary mucinous neoplasm in an academic hospital (2005-2010): what follow-up for unoperated patients? *Pancreas* 2013; 42: 696-700.
- [8] Loizou L, Albiin N, Ansorge C, Andersson M, Segersvärd R, Leidner B, Sundin A, Lundell L and Kartalis N. Computed tomography staging

PET/CT imaging of pancreatitis and old hepatic schistosomiasis

- of pancreatic cancer: a validation study addressing interobserver agreement. *Pancreatology* 2013; 13: 570-575.
- [9] Cassinotto C, Cortade J, Belleannée G, Lapuyade B, Terrebonne E, Vendrely V, Laurent C and Sa-Cunha A. An evaluation of the accuracy of CT when determining resectability of pancreatic head adenocarcinoma after neoadjuvant treatment. *Eur J Radiol* 2013; 82: 589-593.
- [10] Didolkar MS, Coleman CW, Brenner MJ, Chu KU, Olexa N, Stanwyck E, Yu A, Neerchal N and Rabinowitz S. Image-guided stereotactic radiosurgery for locally advanced pancreatic adenocarcinoma results of first 85 patients. *J Gastrointest Surg* 2010; 14: 1547-1559.
- [11] Kauhanen SP, Komar G, Seppänen MP, Dean KI, Minn HR, Kajander SA, Rinta-Kiikka I, Alanen K, Borra RJ, Puolakkainen PA, Nuutila P and Ovaska JT. A prospective diagnostic accuracy study of ¹⁸F-fluorodeoxyglucose positron emission tomography/computed tomography, multidetector row computed tomography, and magnetic resonance imaging in primary diagnosis and staging of pancreatic cancer. *Ann Surg* 2009; 250: 957-963.
- [12] Wang Z, Chen JQ, Liu JL, Qin XG and Huang Y. FDG-PET in diagnosis, staging and prognosis of pancreatic carcinoma: a meta-analysis. *World J Gastroenterol* 2013; 19: 4808-4817.